Topology near the transition temperature in lattice gluodynamics analyzed by low lying modes of the overlap Dirac operator

E.-M. Ilgenfritz
Joint Institute for Nuclear Research, VBLHEP, 141980 Dubna, Russia

B. V. Martemyanov
Institute of Theoretical and Experimental Physics, 117259 Moscow, Russia
National Research Nuclear University MEPhI, 115409, Moscow, Russia
Moscow Institute of Physics and Technology, 141700, Dolgoprudny, Moscow Region, Russia

M. Müller-Preussker
Humboldt-Universität zu Berlin, Institut für Physik, 12489 Berlin, Germany
(Dated: October 1, 2013)

Topological objects of $SU(3)$ gluodynamics are studied near the transition temperature with the help of zero and near-zero modes of the overlap Dirac operator. We construct UV filtered topological charge densities for three versions of temporal boundary conditions applied to this operator, for which zero modes are known to be located on corresponding three types of constituent dyons (antidyons) in the reference case of analytical (anti)caloron solutions. The clusters of the three topological charge densities mark the positions of dyons and antidyons which are also present in equilibrium (Monte Carlo) gluonic fields. We classify them either as constituents of nondissociated (anti)calorons or as constituents of (anti)dyon pairs or as isolated (anti)dyons. The pattern of the Polyakov loop is found in these clusters after a limited number of overimproved cooling steps and resembles predictions from analytical caloron solutions.

PACS numbers: 11.15.Ha, 12.38.Gc, 12.38.Aw
Keywords: Lattice gauge theory, overlap Dirac operator, caloron, dyon

I Introduction

1. Why do we need all this?
2. SU(2) -results
3. First SU(3)-result
4. Analytic caloron solution in SU(2)and SU(3).

II Main part

1. Generation of quantum gauge field configurations.
2. Overlap Dirac operator, its modes and top. charge density.
3. Top. charge clusters and their interpretation.
4. PL pattern in top. charge clusters.

III Conclusion

$$
\begin{aligned}
S[U] \;=\; & \beta \sum_{pl} \frac{1}{3}\mathrm{Re\ Tr}[1 - U_{pl}] \\
& + \; \beta_1 \sum_{rt} \frac{1}{3}\mathrm{Re\ Tr}[1 - U_{rt}] \\
& + \; \beta_2 \sum_{pg} \frac{1}{3}\mathrm{Re\ Tr}[1 - U_{pg}],
\end{aligned}
$$

$$
\beta_1 = -\frac{\beta}{20u_0^2}[1 + 0.4805\alpha] \;, \beta_2 = -\frac{\beta}{u_0^2}0.03325\alpha \;.
$$

$$
u_0 = \left(\langle \frac{1}{3}\mathrm{Re\ Tr}U_{pl}\rangle\right)^{1/4} \qquad \alpha = -\frac{\ln\left(\langle \frac{1}{3}\mathrm{Re\ Tr}U_{pl}\rangle\right)}{3.06839}
$$

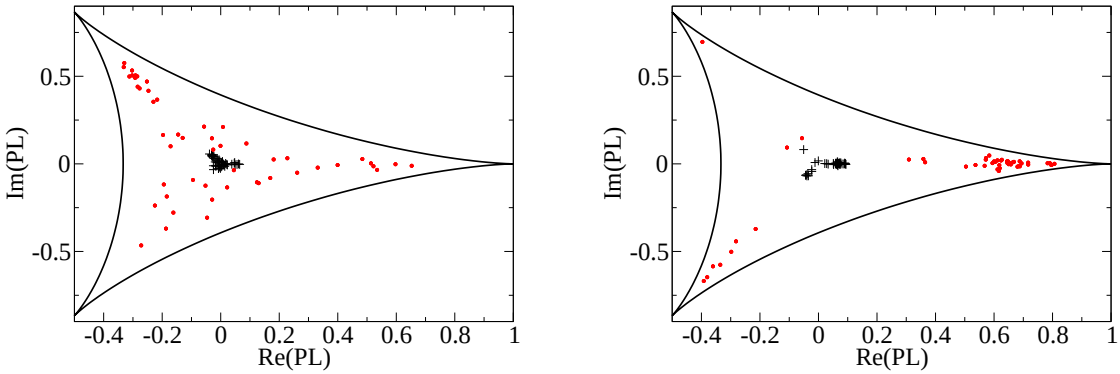

FIG. 1: Scatter plot of the averaged Polyakov loop before (black pluses) and after (red circles) cooling for $\beta = 8.20$ (left) and $\beta = 8.25$ (right).

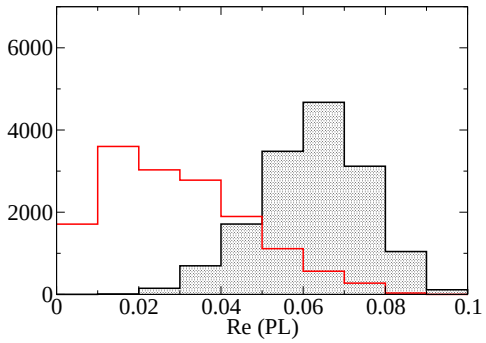

FIG. 2: The distributions of the real part of the averaged Polyakov loop (rotated to the real Z_3 sector) at $\beta = 8.20$ and $\beta = 8.25$ (shadowed), each based on a statistics of 15000 configurations.

$$q_{i,N}(x) = -\sum_{j=1}^{N}\left(1-\frac{\lambda_{i,j}}{2}\right)\psi^{\dagger}_{i,j}(x)\gamma_5\psi_{i,j}(x)\ ,$$

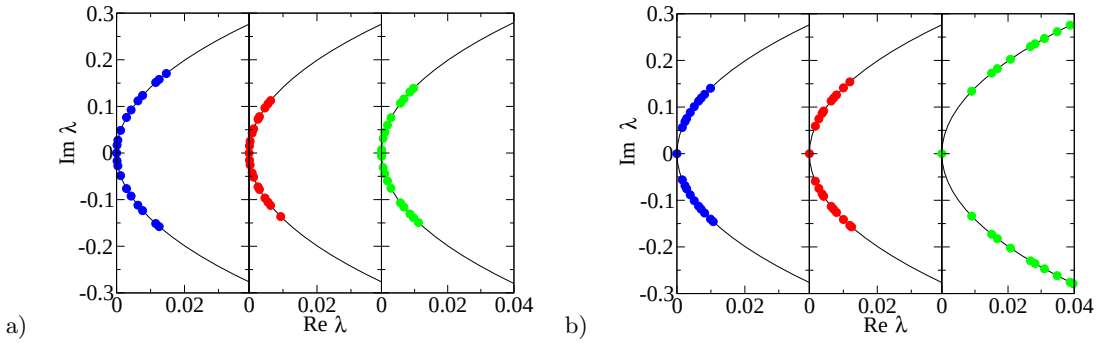

FIG. 3: For three examples of fermion temporal boundary condition the 20 near-zero eigenvalues of the $SU(3)$ overlap Dirac operator are shown, at a) $\beta = 8.20$ and b) $\beta = 8.25$, respectively.

$$N_1 = 869\,, \qquad N_2 = 909\,, \qquad N_3 = 900\,,$$

$$\begin{aligned} \text{number of isolated clusters} &= 1299 \quad (49\%)\,, \\ \text{number of clusters in pairs} &= 782 \quad (29\%)\,, \\ \text{number of clusters in triplets} &= 597 \quad (22\%)\,, \end{aligned}$$

$$N_1 = 1033\,, \qquad N_2 = 1077\,, \qquad N_3 = 886\,,$$

$$\begin{aligned} \text{number of isolated clusters} &= 1600 \quad (55\%)\,, \\ \text{number of clusters in pairs} &= 834 \quad (28\%)\,, \\ \text{number of clusters in triplets} &= 492 \quad (17\%). \end{aligned}$$

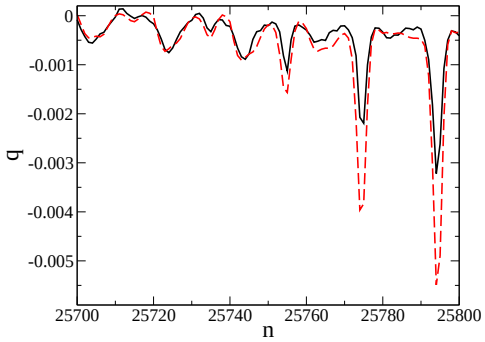

FIG. 4: Comparison (along some string of lattice sites) of the overlap topological charge density of a typical configuration in the confinement phase (averaged over boundary conditions, shown as solid black line) with the gluonic topological charge density (dashed red line). The latter is determined after an optimal number of overimproved cooling steps (see text).

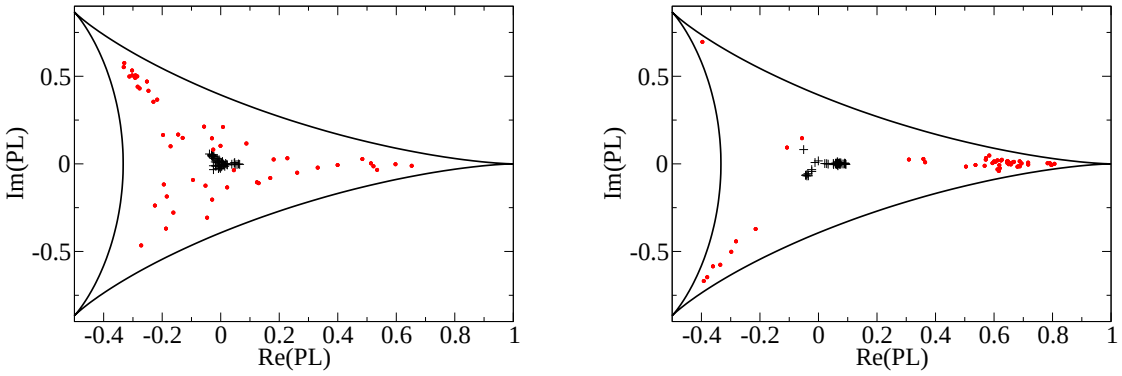

FIG. 5: Scatter plot of the averaged Polyakov loop before (black pluses) and after (red circles) cooling for $\beta = 8.20$ (left) and $\beta = 8.25$ (right).

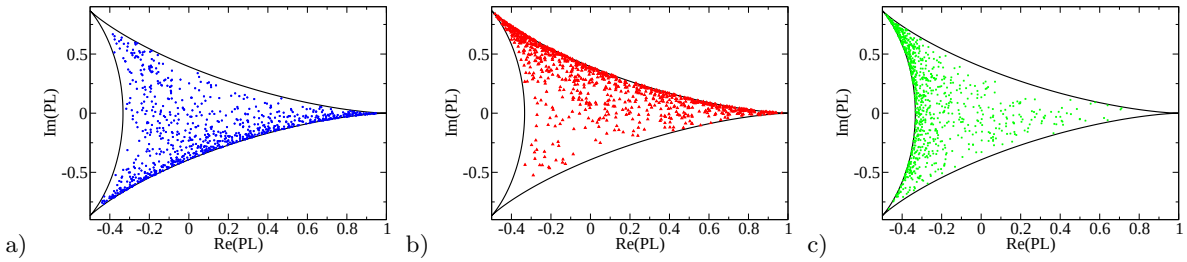

FIG. 6: For three examples of fermion temporal boundary condition, the near-zero modes of $SU(3)$ overlap Dirac operator define three different profiles of the topological charge density on a configuration belonging to the ensemble at $\beta = 8.20$ ($T \simeq T_c$). Each cluster of these profiles is represented in the plots by the Polyakov loop measured in the cluster center. Left: a) 869 clusters of first type (blue stars). Middle: b) 909 clusters of second type (red up triangles). Right: c) 900 clusters of third type (green crosses).

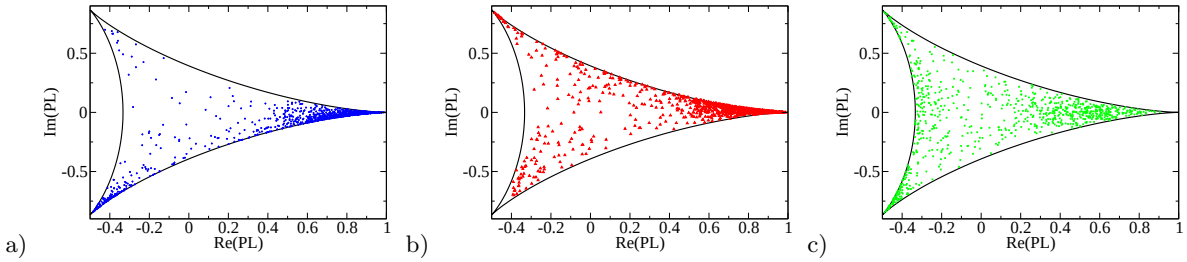

FIG. 7: The same as in Fig. 6a,b,c but for the ensemble at $\beta = 8.25$ ($T \gtrsim T_c$). Left: a) 1033 clusters of first type (blue stars). Middle: b) 1007 clusters of second type (red up triangles). Right: c) 886 clusters of third type (green crosses).

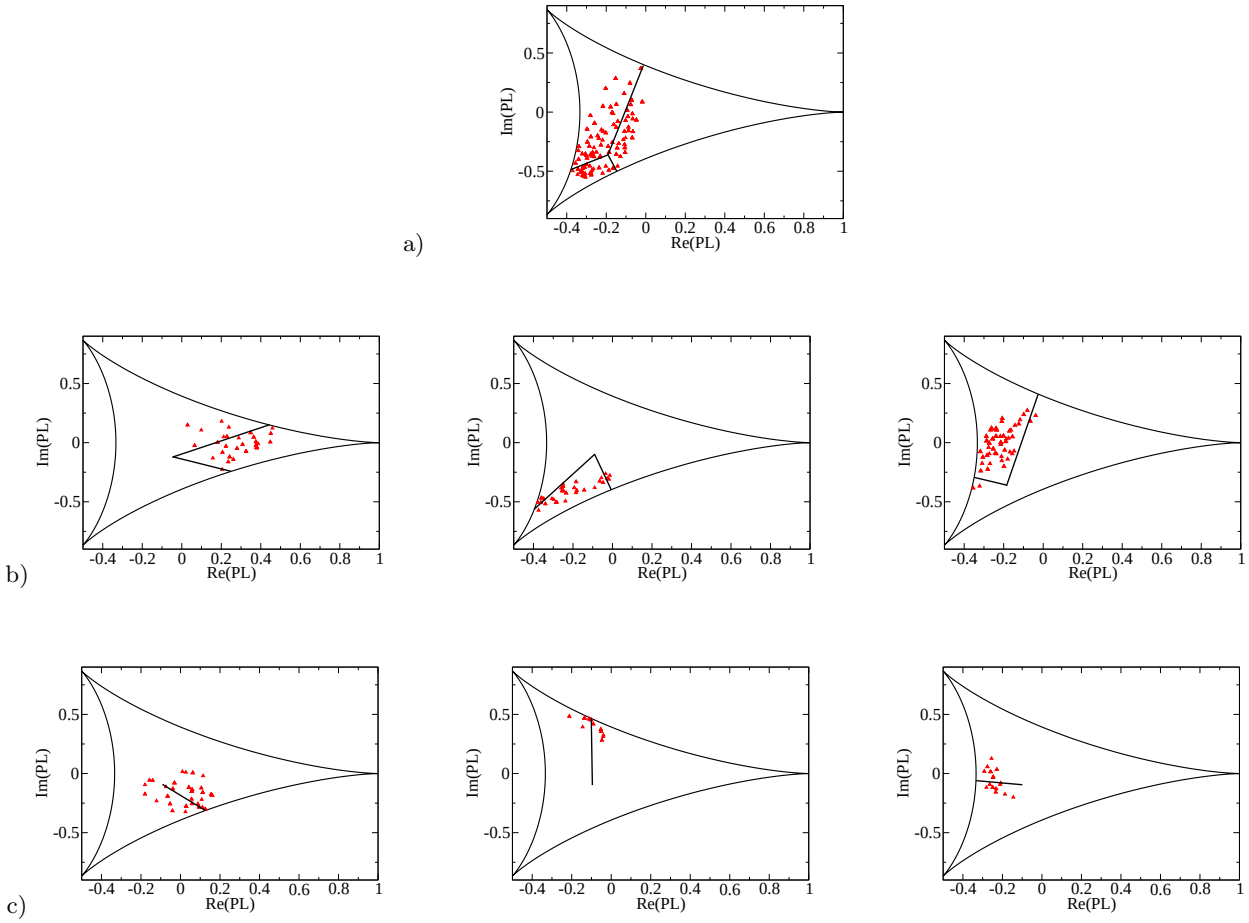

FIG. 8: The profile of Polyakov loop in a) a triplet of clusters (top), b) in three types of cluster pairs (middle) and c) in the three types of isolated clusters (bottom). In the figures straight lines are shown starting from the point representing the averaged Polyakov loop of the cooled configuration and going to a point representing the Polyakov loop in the cluster center.